MATERIALS PHYSICS AND MECHANICS RESEARCH ARTICLE

Submitted: June 29, 2025 Revised: September 1, 2025 Accepted: November 12, 2025

Concrete column performance enhanced by 3D-printed honeycomb, chiral auxetic, and re-entrant lattices via FDM and DLP methods

M. Hematibahar [1], R.S. Fediuk [2,3]✉, N.I. Vatin [4], A. Milani [5], A. Tahmasebi [5], O. Kordi [5], M. Kharun [6], G.R. Fediuk [2], A.O. Shangutov [7], Y.K. Gitman [8]

[1] Department of Architecture, Restoration and Design, RUDN University, Moscow, Russia

[2] Far Eastern Federal University, Vladivostok, Russia

[3] Vladivostok State University, Vladivostok, Russia

[4] Peter the Great St. Petersburg Polytechnic University, St. Petersburg, Russia

[5] Tarbiat Modares University, Tehran, Iran

[6] Moscow State University of Civil Engineering, Moscow, Russia

[7] Perm Military Institute of the National Guard Troops of the Russian Federation, Perm, Russia

[8] Perm State Humanitarian Pedagogical University, Perm, Russian Federation

✉ roman44@yandex.ru

ABSTRACT

This study addresses a gap in the literature by investigating the reinforcement of mini-columns with 3D-printed lattice structures to improve the mechanical performance of cementitious materials for structural applications. Three reinforcement patterns honeycomb, re-entrant auxetic, and chiral auxetic were designed and fabricated using two additive manufacturing methods: fused deposition modeling (FDM) and digital light processing (DLP). Polylactic acid was used for FDM, and photopolymer resin for DLP printing. Each pattern was printed in both cylindrical and hyperboloid geometries and embedded into concrete mini-columns. The objective was to evaluate their influence on compressive strength, flexural behavior, and strain performance. Testing, including ultrasonic pulse velocity, was conducted to assess internal integrity. Results show that the type, placement, and geometry of the reinforcement significantly influenced mechanical performance, with DLP-printed structures providing higher resolution and improved interfacial bonding. Among the patterns, the re-entrant auxetic geometry yielded the highest enhancement in compressive strength up to 18 % compared to unreinforced samples, demonstrating the potential of auxetic designs in structural reinforcement.

KEYWORDS

fused deposition modeling • digital light processing • auxetic structure • spent coffee grounds • peanut shell

Funding. *This research was funded by the Ministry of Science and Higher Education of the Russian Federation within the framework of the state assignment No 075-03-2025-256 dated 16 January 2025, Additional agreement No 075-03-2025-256/1 dated 25 March 2025, FSEG-2025-0008.*

Citation: Hematibahar M, Fediuk RS, Vatin NI, Milani A, Tahmasebi A, Kordi O, Kharun M, Fediuk GR, Shangutov AO, Gitman YK. Concrete column performance enhanced by 3D-printed honeycomb, chiral auxetic, and re-entrant lattices via FDM and DLP methods. *Materials Physics and Mechanics*. 2025;53(5): 164–180. http://dx.doi.org/10.18149/MPM.5352025_14

Introduction

There are different types of reinforced concrete and cementitious materials with fibers, rebar, and other materials [1–4]. There is a new way to reinforce concrete via 3D-printing (3DPRC) [5]. To understand the scope of this field, Wan et al. [6] used a 3D-printed

reinforcement in water, so that when the beam breaks, the self-healing material can repair the concrete. Another example is the 3DPRC under flexural cyclic loading; they found that the maximum crack width was 20–80 μm [7]. Other samples investigated the auxetic cementitious composites (ACCs). They used reinforced cementitious materials with four types of auxetic patterns: "re-entrant" (RE), "rotating-square" (RS), "chiral" (CR), and "missing-rib" (MR). They understand RE has 853 % highest ductility. Moreover, if the water-to-binder ratio decreased from 0.4 to 0.3, then the compressive strength increased by more than 18.5 % [8]. Salazar et al. [9] reinforced an ultra-high-performance concrete (UHPC) beam with a 3D printed lattice. It has been observed that certain types of ultra-high-performance concrete (UHPC) reinforced with 3D-printed lattice structures exhibit higher compressive and flexural strengths than other samples. The literature review aims to present the current state of 3D-printed reinforced concrete (3PRC) technology. Although still emerging, this technology shows significant potential for enhancing performance in both civil engineering and materials science applications. At the same time, substantial efforts have been directed toward optimizing its structural performance and fabrication processes.

To find the best pattern and shape for a concrete beam, Hematibahar et al. [10] first added a hyperboloid structure to concrete to determine its compressive, tensile, and flexural strengths. They found that the hyperboloid shell structure cannot affect tensile strength; however, it does affect concrete strain. Later, the concrete beam was optimized using various 3D-printed truss types. They printed four types of trusses (Pratt, Howe, Warren, and Warren with vertical members) with the fused deposition modeling (FDM) technique. Reinforced concrete with a 3D-printed Warren truss increased in flexural strength by more than 18 %. Although the flexural strength of the beam increased with the addition of Warren trusses to concrete, the strain condition was strain-softening [11]. Finally, Hematibahar et al. [12] find optimized strain-hardening 3DPRC. They reinforced cementitious materials with honeycomb, 3D honeycomb, grid, and triangle at different distances from the bottom of the cementitious beam. Overall, they found that although the triangle and 3D-printed reinforced cementitious improved flexural strength more than the control sample, the Honeycomb pattern increased the beam's flexural strength and changed the reinforced cementitious's strain behavior to strain-hardening. Therefore, pattern, distance, and placement method are the best ways to choose the real pattern. Most studies focused on changing the concrete bearing and capacity in "concrete or cementitious beam". For example, Xu et al. [13] analyzed different types of 3D-printed reinforced concrete with a mesh pattern under three-point bending of a concrete beam. In another example, Meng et al. [14] investigated a special geometry with auxetic behavior in both in-plane and out-of-plane directions, resulting in a 1.7 times higher compaction energy than that of conventional cement-based materials. Finally, the current research focused on improving the compressive and flexural strength of concrete beams, either by creating new theories or by filling scientific gaps. To fill the gap of previous studies, this paper decides to reinforced the mini column for the first time after optimize the pattern and distance in the cementitious beam.

This article endeavors to reinforce the cementitious beam using four three-pattern types (honeycomb, re-entering auxetic (RE), chiral auxetic (CA). This study aims to conduct extensive research on cyclic loading, reinforced beams, and tension beams. Also, the

current study aimed to examine mechanical properties, including compression testing for each reinforced type, and to conduct nondestructive tests.

Material and Methods

Materials

Table 1 illustrates the mixture design of the concrete samples used in this study. The components were cement, water, marble powder, straw powder, microsilica, and superplasticizer (SP). Table 2 presents the microsilica chemical composition derived from X-ray fluorescence (XRF) analysis. This analysis was examined using a Philips PW 2404 device.

Table 1. Mixture design for samples in this study (kg/m^3)

Cement	Water	Marble powder	Straw powder	Microsilica	SP
500	154	1400	100	100	12.32

Table 2. Microsilica chemical composition (wt. %).

SiO_2	91.55
Al_2O_3	1.024
K_2O	1.73
MgO	1.02
Na_2O	0.52
Fe_2O_3	0.59
CaO	0.45
SO_3	0.35
P_2O_3	0.14
Cl	0.105
MnO	0.074
Zn	0.014
Pb	0.009
Rb	0.005
Sr	0.005
Cu	0.003
Ga	0.002
L.O.I	2.37

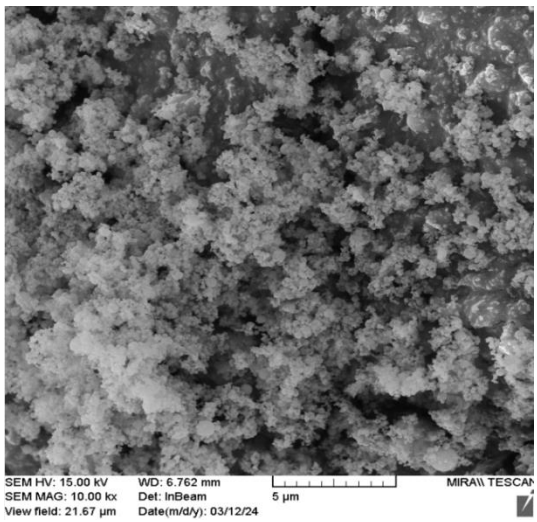

Fig. 1. Scanning electron microscopy (SEM) image of microsilica microstructure

Marble powder can help mitigate many environmental hazards, such as air pollution [15]. In addition, 10 % of marble added to cementitious materials increases the compressive strength [16] (Fig. 1). Microsilica (silica fume) can increase the calcium silicate hydrate (CSH) formation process in the hydration time. For example, some studies added silica fume to cement and found that it can improve concrete compressive strength by rapidly increasing CSH formation [17]. In another experiment, Shooshpasha et al. [18] found that silica fume can fill voids in cement paste and increase the material's durability. Superplasticizer can reduce water content and improve the mechanical properties of concrete [19]. SP affected the concrete compressive strength and other mechanical properties [20].

Methods

Etymology. In this project, researchers aim to test a new engineering method that will make it easier for engineers to build columns in the future. Hence, this team introduced this technology to the world for the first time and selected the name "Sotun" for it. "Sotun" is the Persian translation of "column" in English. Since it is difficult to repeat the "Sotun" word, the project will be called STN.

FDM and DLP methods. There are two types of 3D primary samples, using FDM (fused deposition modeling) and DLP (digital light processing). DLP enables the automated production of customized 3D parts using digital models. This technology has played an important role in industries such as aerospace, medicine, design, and engineering over the past 40 years. High accuracy in DLP can be achieved by selecting appropriate process parameters (such as layer thickness, printing direction, curing time and temperature, and laser power) and suitable materials. This study investigates the effects of these parameters on mechanical properties, including tensile strength, hardness, and surface roughness [21]. DLP is a precision 3D printing technology that uses an ultraviolet (UV) laser to solidify a liquid photopolymer resin layer by layer (Table 3). This process causes localized polymerization and the formation of complex structures by controlled laser irradiation into the resin reservoir. DLP is particularly used in the production of prototypes and industrial parts due to its high precision and excellent surface finish. Parameters such as laser power, layer thickness, and curing temperature directly affect the quality of the final product [22].

Table 3. Parameters of 3D-printed samples for DLP method

Printing resolution, mm	Infill, %	Exposure time, s
0.05	100	2.5

Rapid prototyping is done with technologies such as 3D printing and additive manufacturing. In additive manufacturing, materials are layered on top of each other to create the final product. One of the most widely used methods in this field is FDM, in which the selection of process parameters, such as temperature and speed, directly affects the quality of the manufactured parts. This method is expanding day by day across industries and research, especially in PLA-based applications, due to its advantages such as low cost, high quality, and short production time [23].

3D-printed samples were fabricated using Quantum 3D printer with the following printing parameters: nozzle diameter of 0.4 mm, raster width of 0.6 mm, layer height of 0.3 mm, and 100 % infill (Table 4). Creality PLA+ filament was used for all prints. Due to the complexity of the sample geometries, extensive support structures were required during printing and were carefully removed afterward. The samples consisted of two general shapes: cylindrical and hyperboloid cylinders with a 5-degree angle from the vertical axis. Each shape featured three different wall patterns: honeycomb, chiral auxetic, and re-entrant.

Table 4. Parameters of 3D-printed samples for FDM method

Nozzle diameter, mm	Printing speed, mm/s	Layer height, mm	Infill, %	Raster diameter, mm
0.4	30	0.3	100	0.6

3D-printing pattern. In this study, three types of reinforcement patterns, honeycomb (HC), re-entrant auxetic (RE), and chiral auxetic (CA) were used to fabricate mini columns via 3D-printing. Each pattern was designed in both cylindrical and hyperboloid geometries. Figure 2 illustrates the pattern types, their geometrical configurations, and the corresponding printed structures.

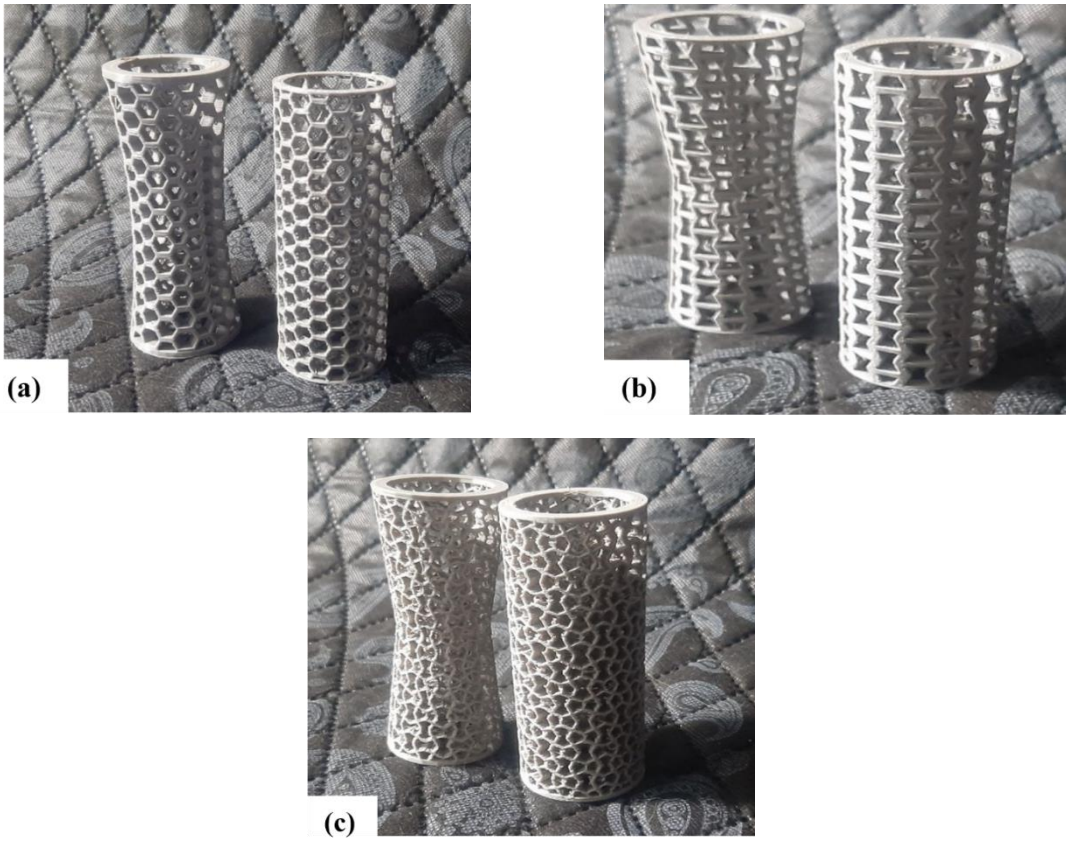

Fig. 2. Reinforcement pattern types used in this study: (a) honeycomb (HC), (b) re-entrant auxetic (RE), and (c) chiral auxetic (CA), each shown in both cylindrical and hyperboloid geometries

Each reinforced 3D print is divided into two samples: the hyperboloid with an 85° angle and the cylinder. The 85° specimens were created to understand the hyperboloid behavior with maximum effect under compressive loading. The diameter of each mini

column is 5.5 cm, and its height is more than 11 cm. According to Fig. 2, the 3D-printed reinforcement had a 1.5 cm cover over the external cementitious materials.

Figure 3 shows the research method. Firstly, the cementitious materials were mixed by hand until the mixture was ready for embedding in the molds. Finally, three types of reinforcement were placed in the molds, and cementitious material was embedded within them.

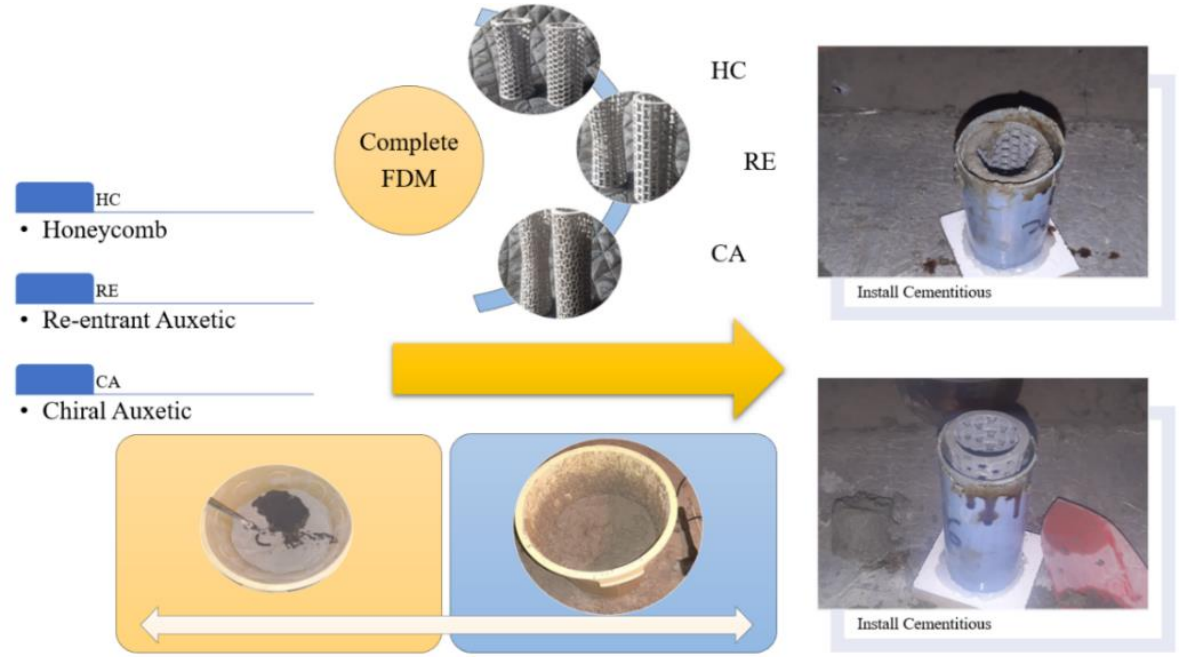

Fig. 3. Step-by-step process of embedding 3D-printed reinforcement structures into concrete molds for mini-column fabrication

Experimental methods. To determine the mechanical properties of concrete and mini-columns, as well as to conduct nondestructive testing, the following specimens were tested (Fig. 4): concrete 5 × 5 × 5 cm^3 cubes according to ASTM C109 [24]; reinforced cement columns under compressive loading according to ASTM C39/C39M-21 [25].

The following tests were carried out: displacements at three points of the columns, recorded by sensors installed at these three points to detect buckling; compressive strength of each specimen according to ASTM C39/C39M-21 [25].

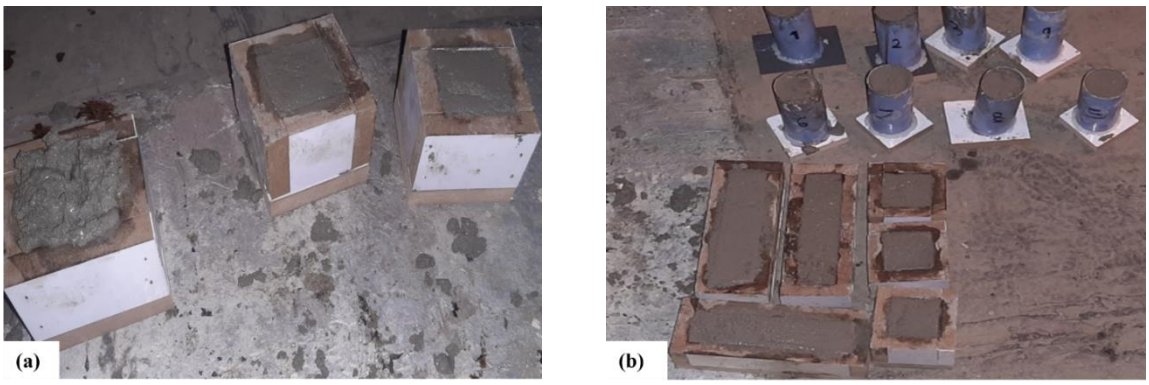

Fig. 4. (a) Cubical (5 × 5 × 5 cm^3) and rectangular concrete specimens prepared as reference samples; (b) specimens placed under standard curing conditions

Results and Discussion

In this section, three cases were investigated: the compressive strength of the control sample, the reinforced concrete column using the FDM method, and the reinforced concrete column using the DLP method.

Compressive strength

The structure formation of composite concrete columns with 3D-printed inclusions (honeycombs, chiral auxetics, and re-entrant lattices) occurs through the formation of a hierarchical internal architecture, where polymer metastructures manufactured using FDM or DLP methods act as permanent formwork or a deformation framework that determines the spatial organization of the stress-strain state in the hardening concrete. The cell geometry determines local zones of stress concentration and redistribution, and interfacial interactions at the polymer-cement stone boundary affect the integrity and crack resistance of the system. However, full structural formation is limited by the incompatibility between the physical and mechanical properties of the components and the lack of chemical adhesion, which requires further optimization of the compositions and co-printing technologies.

The compressive strength of the control specimen is 113 MPa; in fact, the control specimen was reinforced without any pattern. This high strength, which is twice that of traditional concrete, opens the broadest prospects for the development of these materials.

FDM Method

This section presents the result of concrete reinforcement using FDM method.

CA samples. Considering Fig. 5, if the CA sample is used as the reinforced sample, the compressive strength decreased at 85 and 90 degrees. Figure 5(a) shows that the compressive strength increases to a point where it reaches its maximum value (84.91 MPa). After reaching the maximum compressive strength, the material fails, and the strength decreases. Changes in the slope of the graph can indicate structural changes or internal cracks in the material. Figure 5(b) shows a compressive strength of 105.58 MPa. According to Fig. 5(b), the influence of 3D-printed reinforcement is observed.

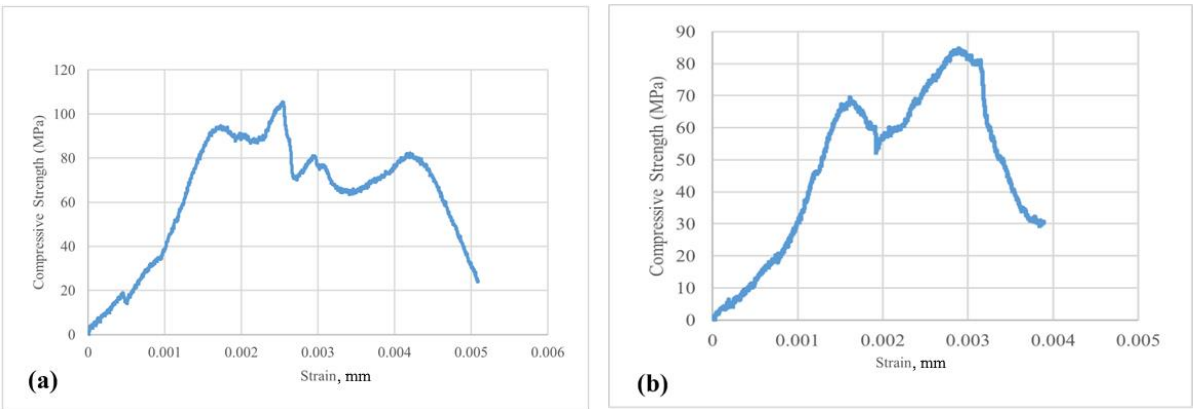

Fig. 5. CA sample. (a) CA85, (b) CA90

HC sample. According to Fig. 6, the compressive strength of the samples increased by more than 50 % for both types of reinforced concrete mini columns. In fact, according to Fig. 6, the compressive stress-strain curve of HC85 shows less strain hardening than that of HC90.

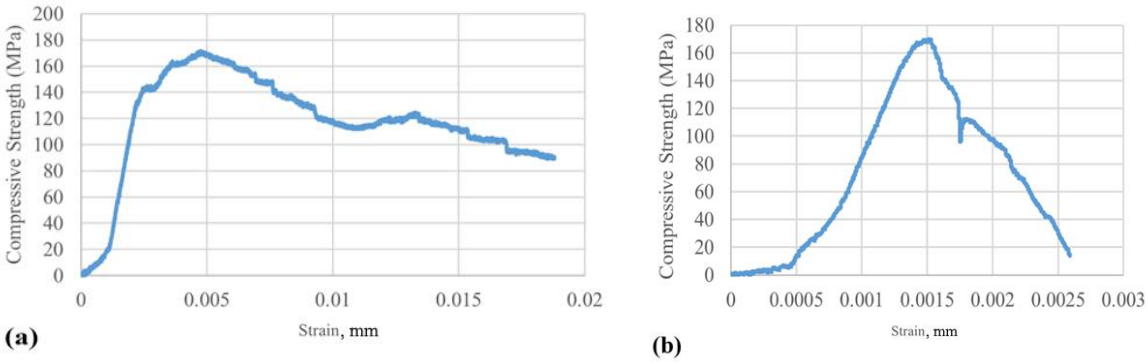

Fig. 6. HC sample: (a) HC85, (b) HC90

Carefully studying Fig. 6, we note some interesting features. Columns with honeycomb reinforcement are much more effective than columns with chiral auxetic reinforcement for two reasons. First, they show up with compressive strengths up to 2 times higher. Second, a much smaller degree of dependence of compressive strength on the angle of inclination of reinforcement in columns is noted (171 MPa for 85 degrees and 169 MPa for 90 degrees).

RE Sample. According to Fig. 7, if re-entrant (RE) reinforcement is added to concrete, the compressive strength increases by more than 267 % for RE with 85 degrees and 77 % for RE with 90 degrees.

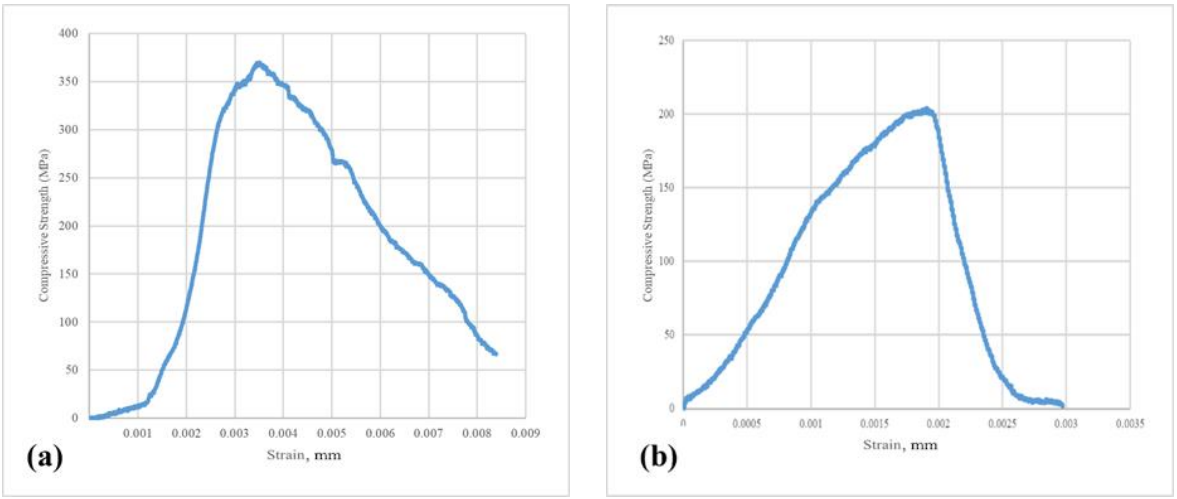

Fig. 7. RE sample: (a) RE85, (b) RE90

This reinforcement can be considered the most effective type compared to chiral auxetic and honeycomb reinforcements. Achieving a high compressive strength (369 MPa) enables these columns to be used in the most heavily loaded and critical structures. On the other hand, there is a significant spread in compressive strength values

of 170 MPa (from 369 to 199 MPa) if the column reinforcement angle is changed by 5 degrees (from 85 to 90 degrees).

The compressive strength of all samples except HC-90, HC-85, and CA-90 is lower than that of the other samples. Considering Fig. 6, if concrete is reinforced with RE-90, the concrete compressive strength improved by more than 42 % compared to the control sample. Moreover, if concrete is reinforced with 25 %, its compressive strength will improve.

However, in the previous structures, the reinforced concrete beam was found to be the rational type, as concrete beams are honeycombed structures. This study found that the sensible way to reinforce concrete columns is with RE90 and CA85 concrete. RE type of concrete known as "re-entrant" and CA type of concrete known as "chiral". The use of honeycomb-reinforced CA concrete can significantly alter column properties. The CA form can change the concrete from compressive to tensile and can also reduce its tensile strength. Hence, all types of concrete, if reinforced with concrete by CA at an angle of 85 degrees [26]. Therefore, adding CA to concrete can increase the compressive strength at 85 degrees, but at 90 degrees, the compressive strength decreased to 87 MPa.

Understanding the re-entry structure is very important because the structure must be re-entered (RA). In this type of structure, it is essential to observe the energy dissipation [27]. According to the combination of Figs. 7 and 9, if RE was washed for less than the special amount (the less-than-control sample), the STN improved by more than 42 %. However, if RE was reinforced with 90°, the STN improved by more than 42 %. In fact, the cement must increase the concrete's plasticity (Fig. 8). This ratio is also the same for Chorial too [28]. Different types of materials must be used. First, there are organic materials such as cellulose Nanocrystals, Inorganic materials such as gusted twisted, and organic-inorganic materials such as protein MOF [29].

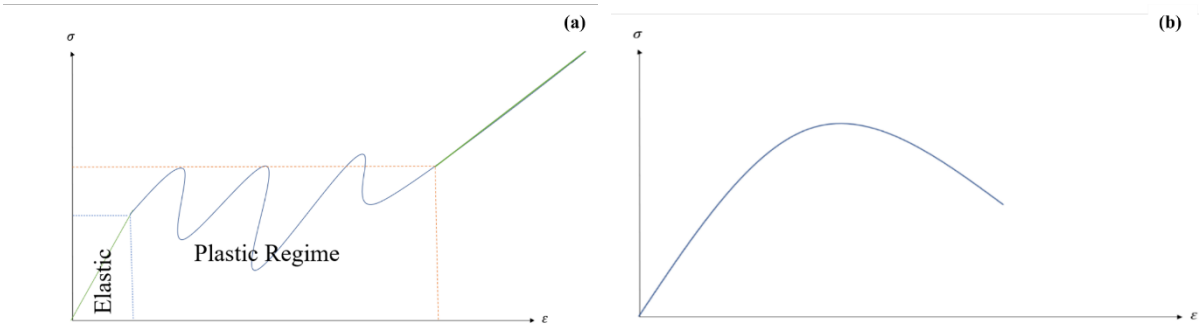

Fig. 8. Stress-strain curve of (a) RE under compression, (b) concrete

Considering the current study, horizontal resistance (F_y) can be considered in three conditions:

$$F_y = \left\{ \begin{matrix} Concrete.stiffnes.has.to.be.more.than.Plastic.system. \\ Concrete.stiffnes.is.equal.with.Plastic.system. \\ Concrete.stiffnes.is.less.than.Plastic.system. \\ \vdots \end{matrix} \right\}. \quad (1)$$

Considering the investigation, the algorithmic system of this article was based on Eq. (1). To find the best form of compressive stiffness of concrete, it has to be greater than the plastic system (RE90, RE85, and CA85). Moreover, if the system had been

balanced, the RE85 configuration would have been appropriate. As shown in Fig. 7, conventional concrete must improve the failure resistance of the specimen without inducing additional brittleness [30,31]. Considering Fig. 6, the conventional concrete has been cracked in shear types. Moreover, RE, HC, and RC had resistance against concrete, whereas shear compressive. Other elements illustrate torsional strength; it means that shear strength changes to twisting.

CA cracked hardly and assisted concrete very soon; overall, concrete, CA, and cementitious materials show complete failure. Overall, 90 degrees is better than 85 degrees. The most interesting situation is twisted concrete from compressive strength and shear conflicts. Meanwhile, twisted reinforced concrete. Overall, the maximum indexes were pattern, degree of pattern, negative possessions, etc.

DLP samples

In this section, the reinforced concrete fabricated using the DLP method is investigated.

CA samples. According to Fig. 9, the compressive strength has improved by more than 326 % for DLP method and CA shape with a 90-degree hyperboloid. For specimen CA90, the reinforcement is directly engaged, whereas in CA85 the concrete is first subjected to compressive loading.

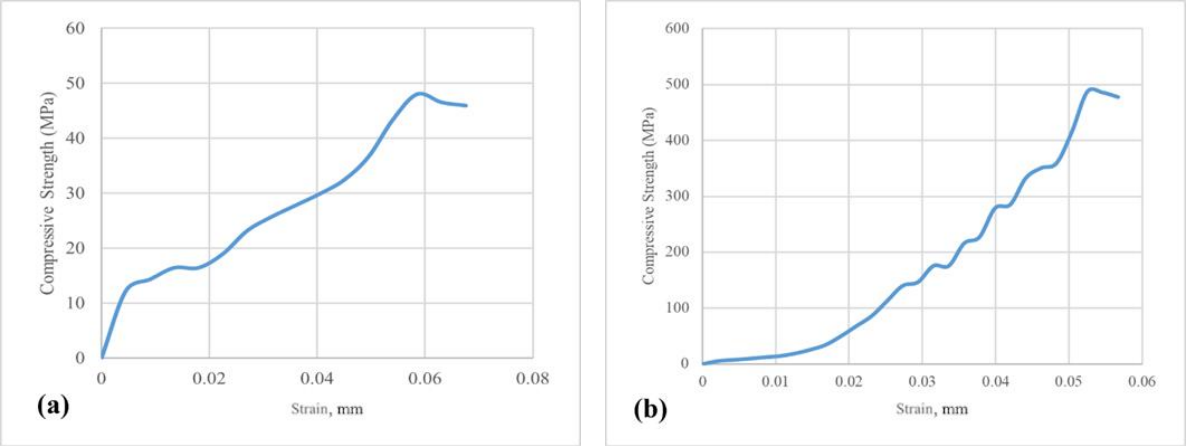

Fig. 9. CA sample: (a) CA85, (b) CA90

In the additive manufacturing of SA reinforcement using DLP methods, the most interesting feature is the strength under compression of the columns. Firstly, the maximum compressive strength of 488 MPa is achieved at a reinforcement angle of 90 degrees. On the other hand, if the angle is reduced by 5 degrees, the compressive strength decreases by an order of magnitude (48 MPa). This decrease necessitates careful design and strict control of reinforcement quality.

HC Sample. Considering Fig. 10, the compressive strength decreased for HC90 and improved for HC85. However, DLP-printed samples for honeycomb reinforcement are twice as effective (in terms of compressive strength) as FDM-printed samples. This effectiveness suggests the importance of the research results presented in this article, which confirm the difficulty of predicting the achievement of target compressive-strength values using various additive technologies to produce reinforcement cages of different geometries.

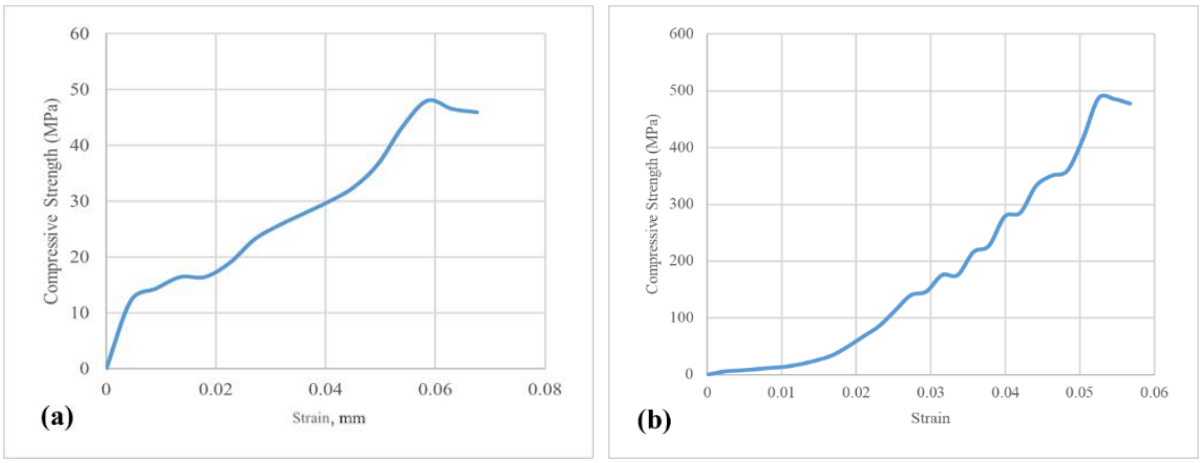

Fig. 10. HC sample: (a) HC85, (b) HC90

RE Samples. According to Fig. 11, the compressive strength increases by more than 30 % compared to conventional concrete samples. Despite the lower results compared to FDM, it is worth noting the lower dependence on the reinforcement angle (142 and 139 MPa at 85 and 90 degrees, respectively).

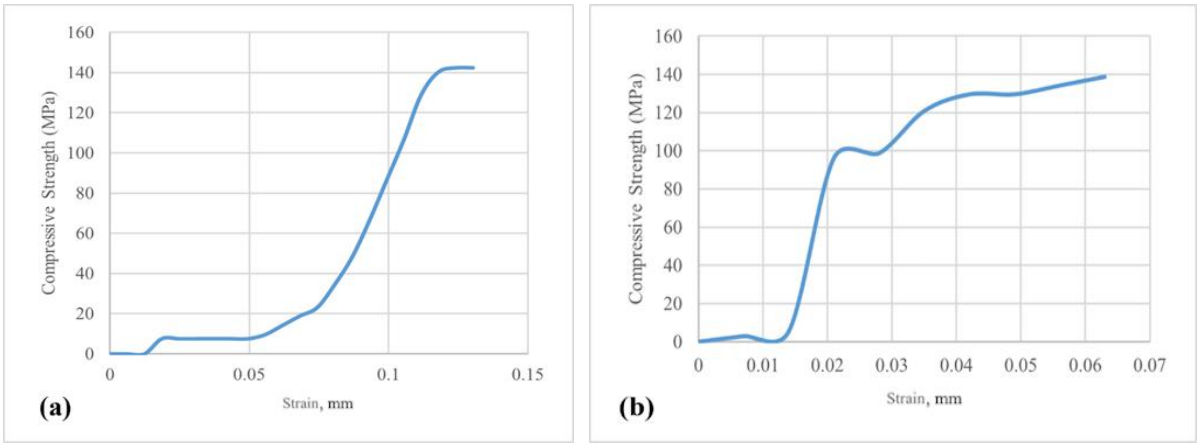

Fig. 11. RE sample: (a) RE85, (b) RE90

Failure types

This part drives to two sections; the first part is about the failure of all samples. Moreover, the second part is nondestructive testing for buckling STN.

Failure types of concrete. Two types of concrete failure have been shown in Fig. 12: the cube surface has been separated, and the next layer of concrete has failed. In STN columns, if different types of concrete have failed under compression, first the concrete cover separated, and then the maximum tension was on the inside of the reinforced concrete. Moreover, reinforced concrete prevents shear cracks (Fig. 13(c,d,e). Figure 13(c) illustrates most of the concrete locked into the STN, Honeycomb structure. It should be understood that if reinforcement with different types of concrete, such as Honeycomb and other structures, is added, it shows better deformations and higher energy (85 degrees) than other (90 degrees).

Golias et al. [32] studied the carbon FRP column cladding of reinforced concrete beams under cyclic loading and found that, if the column was reinforced with CFRP cladding, shear cracks increased. Chandramouli et al. [33] used fiber-reinforced concrete and a hybrid double-skin tubular column within concrete. They analyzed the fiber angle and fiber thickness of the concrete tube. The results show that as fiber thickness and steel increased, compressive strength improved. Overall, stripping reinforced columns away from concrete columns can increase the compressive strength; at the same time, concrete falls till concrete. The concrete in the tension and pressure zones cracks, not only in columns, but also in beams, when loads are applied [34].

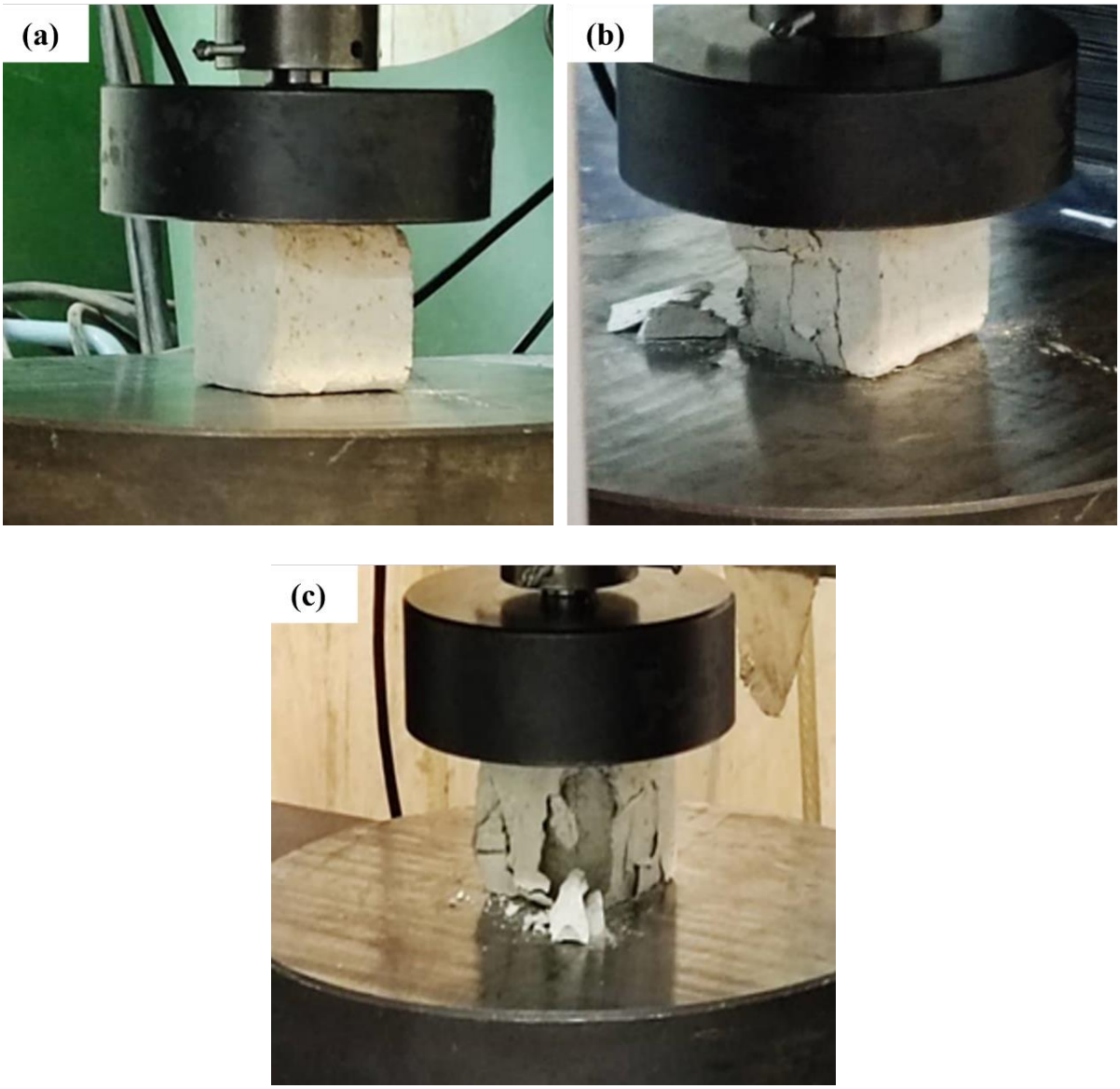

Fig. 12. Compression the cube samples: (a) cube samples under loading; (b) under loading and cracking; (c) failure of cube samples

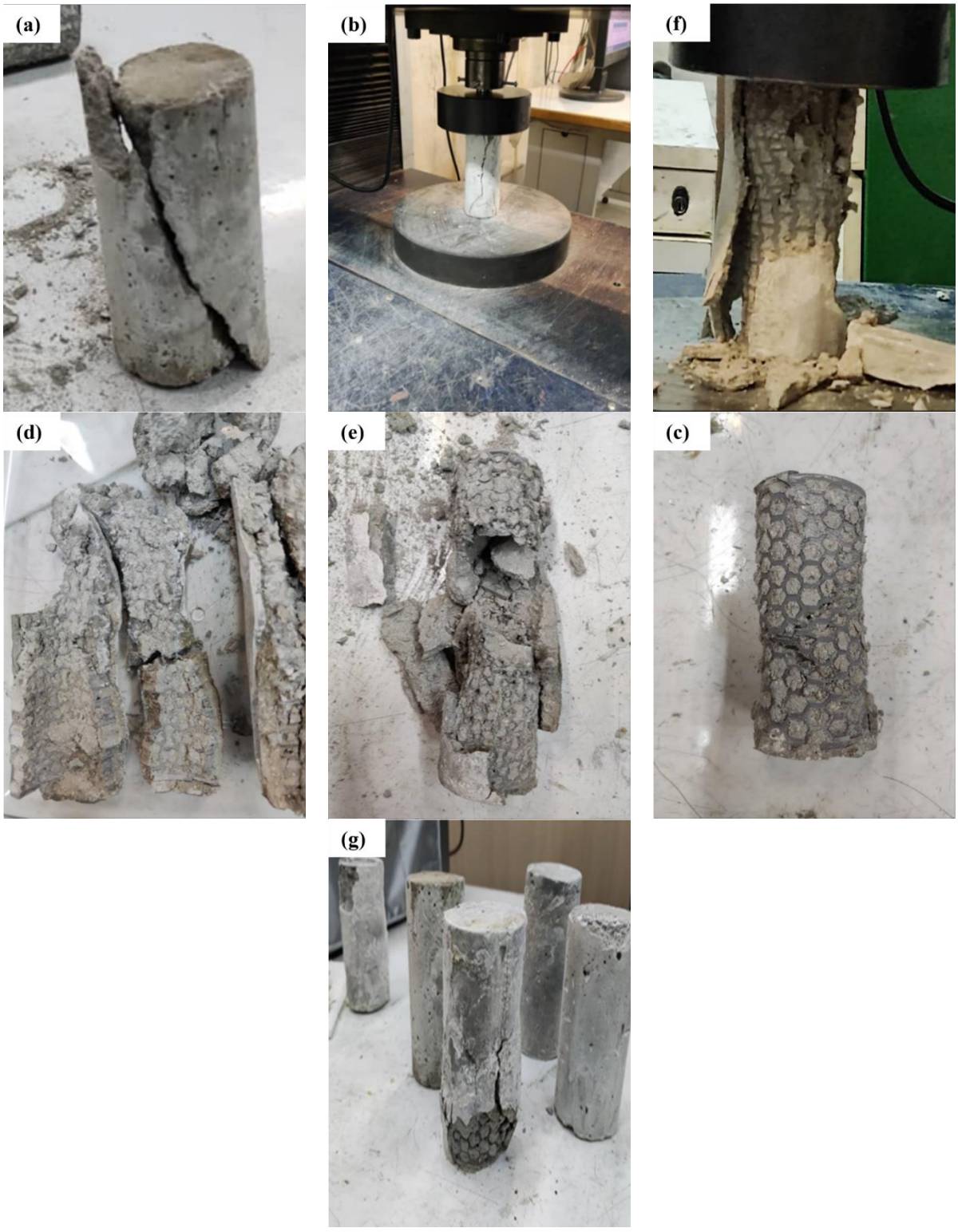

Fig. 13. Failure of STN concrete; (a) control sample;(b) control sample; (c) honeycomb; (d) different of styles of reinforced concrete; (e) RE-85; (f) CA-90; (g) failures of different concrete samples

Summary of results

This study investigated the effect of 3D-printed reinforcement patterns, including honeycomb, recursive auxetic, and chiral auxetic structures, on the mechanical performance of small concrete columns. The findings indicate significant differences in

compressive strength, failure modes, and strain behavior based on the geometry and location of the reinforcements. The results are discussed in the context of previous research and practical applications.

The RE pattern, especially the RE85 and RE90 specimens, showed the greatest improvement in compressive strength (267 and 77 %, respectively). These results are consistent with previous studies that emphasized the high energy absorption and ductility of eutectic structures under compression [27]. The uniform stress distribution in the recursive geometry is likely responsible for this improvement. In contrast, the CA pattern produced different results: the CA85 specimen increased strength by 165 %, while the CA90 specimen decreased it. These results suggest that the angle of reinforcement placement (85° vs. 90°) plays a key role in load carrying, probably due to differences in stress redistribution and buckling resistance [26]. The honeycomb (HC) pattern, which performed well in previous studies on beams [12,30], showed a moderate improvement (50 %) in columns. This difference highlights the importance of the specific design of stiffeners for different structural elements (beams vs. columns) and loading conditions.

The 85° hyperbolic design performed better than the 90° cylindrical specimens in all models (RE85 vs. RE90). This result supports the hypothesis that angled reinforcements are better able to restrain shear stresses and delay crack propagation, as observed in hyperbolic shell structures [10]. The failure modes also confirmed that the 85° reinforced columns had a more ductile behavior, whereas the 90° columns failed abruptly due to localized shear cracks.

The DLP-printed CA90 specimen showed a significant increase of 326 % in compressive strength, which was much higher than that of the FDM-printed specimens. This result indicates the influence of printing accuracy and material density on structural performance. The high accuracy of DLP probably maintains the integrity of the eutectic geometry better under load. However, the HC and RE patterns in the DLP method showed less improvement, indicating that material brittleness or adhesion between concrete and DLP polymers may need to be optimized [30].

Destructive tests showed that the reinforced columns had greater resistance to shear cracking than the control specimens. For example, the HC pattern confined the concrete within its cells, preventing complete collapse. These findings are consistent with studies on FRP-reinforced columns [32,34], but 3D-printed reinforcements offer greater design flexibility and environmental benefits. For example, eutectic patterns can reduce material consumption while maintaining strength, which is consistent with sustainable construction goals [16,35-46].

This study focused on small columns; generalizing the results to real columns requires further investigation of printability and cost-effectiveness. Long-term durability under cyclic loading and environmental conditions (such as humidity and temperature) needs to be tested. Future research could explore hybrid reinforcements or multi-material printing to improve surface adhesion.

The production and implementation of these mini-columns in large-scale construction open up broad prospects for the development of small businesses in the regions, consistent with earlier studies.

Although the use of 3D-printed auxetic and re-entrant structures for strengthening concrete columns demonstrates promising mechanical properties (increased impact

strength, negative Poisson's ratio, and controlled deformation), their practical implementation in construction practice is currently limited by technological, economic, and regulatory barriers. Future research should focus on scalability, material compatibility, and standardization to translate these innovations from the laboratory to the construction site.

Conclusions

This study provides valuable insights into the use of 3D-printed reinforced concrete (3PRC) to enhance the mechanical properties of mini-columns. The investigation of three distinct reinforcement patterns, namely honeycomb (HC), re-entrant auxetic (RE), and chiral auxetic (CA), shows that the geometry and placement of reinforcement significantly influence the performance of cementitious materials under compression and flexural loads. The results demonstrated that RE90 and CA85 reinforcement patterns increased the compressive strength of the concrete by more than 40 % compared to the control sample, with RE90 showing the greatest improvement. On the other hand, HC-90 and CA90 patterns resulted in lower compressive strength, highlighting the importance of selecting optimal patterns for reinforced concrete structures. Nondestructive testing and failure analysis revealed that reinforced columns exhibited greater resistance to shear cracking and improved energy absorption. This study fills a gap in existing research by focusing on optimizing 3D printing techniques for concrete reinforcement, specifically for mini-columns. The study offers practical implications for the design of more efficient, durable, and sustainable concrete structures in future civil engineering applications.

CRediT authorship contribution statement

Mohammad Hematibahar: writing – review & editing, writing – original draft; **Roman S. Fediuk**: conceptualization, writing – original draft; **Nikolai I. Vatin**: investigation, writing – original draft; **Amirali Milani**: supervision, writing – original draft; **Ahmadreza Tahmasebi:** data curation, writing – original draft; **Omid Kordi**: writing – review & editing, writing – original draft; **Makhmud Kharun**: conceptualization, writing – original draft; **German R. Fediuk**: investigation, writing – original draft; **Anton O. Shangutov**: supervision, writing – original draft; **Yelena K. Gitman**: data curation, writing – original draft.

Conflict of interest

The authors declare that they have no conflict of interest.

References

1. Vatin NI, Hematibahar M, Gebre T. Impact of Basalt Fiber Reinforced Concrete in Protected Buildings: A Review. *Frontiers in Built Environment*. 2024;10: 1407327.
2. Momeni K, Vatin N, Hematibahar M, Gebre T. Repair Overlays of Modified Polymer Mortar Containing Glass Powder and Composite Fibers-Reinforced Slag: Mechanical Properties, Energy Absorption, and Adhesion to Substrate Concrete. *Frontiers in Built Environment*. 2024;10: 1479849.

3. Hematibahar M, Kharun M, Beskopylny A, Stel'makh S, Shcherban E, Razveeva I. Analysis of Models to Predict Mechanical Properties of High-Performance and Ultra-High-Performance Concrete Using Machine Learning. *Journal of Composites Science*. 2024;8: 287.
4. Chiadighikaobi PC, Hematibahar M, Kharun MA, Stashevskaya N, Camara K. Predicting Mechanical Properties of Self-Healing Concrete with Trichoderma Reesei Fungus Using Machine Learning. *Cogent Engineering*. 2024;11: 2307193.
5. Hematibahar M, Hasanzadeh A, Kharun M, Beskopylny AN, Stel'makh SA, Shcherban' EM. The Influence of Three-Dimensionally Printed Polymer Materials as Trusses and Shell Structures on the Mechanical Properties and Load-Bearing Capacity of Reinforced Concrete. *Materials*. 2024;17(14): 3413.
6. Wan Z, Xu Y, Zhang Y, He S, Šavija B. Mechanical Properties and Healing Efficiency of 3D-Printed ABS Vascular Based Self-Healing Cementitious Composite: Experiments and Modelling. *Engineering Fracture Mechanics*. 2022;267: 108471.
7. Sun R, Han L, Zhang H, Ge Z, Guan Y, Ling Y, Schlangen E, Šavija B. Fatigue Life and Cracking Characterization of Engineered Cementitious Composites (ECC) under Flexural Cyclic Load. *Construction and Building Materials*. 2022;335: 127465.
8. Xu Y, Savija B. Auxetic Cementitious Composites (ACCs) with Excellent Compressive Ductility: Experiments and Modeling. *Materials & Design*. 2024;237: 112572.
9. Salazar B, Aghdasi P, Williams ID, Ostertag CP, Taylor HK. Polymer Lattice-Reinforcement for Enhancing Ductility of Concrete. *Materials & Design*. 2020;196: 109184.
10. Hematibahar M, Hasanzadeh A, Vatin N, Kharun M, Shooshpasha I. Influence of 3D-Printed Reinforcement on the Mechanical and Fracture Characteristics of Ultra High-Performance Concrete. *Results Eng*. 2023;19: 101365.
11. Chiadighikaobi PC, Hasanzadeh A, Hematibahar M, Kharun M, Mousavi MS, Stashevskaya NA, Adedapo Adegoke M. Evaluation of the Mechanical Behavior of High-Performance Concrete (HPC) Reinforced with 3D-Printed Trusses. *Results Eng*. 2024;22: 102058.
12. Hematibahar M, Milani A, Fediuk R, Amran M, Bakhtiary A, Kharun M, Mousavi MS. Optimization of 3D-Printed Reinforced Concrete Beams with Four Types of Reinforced Patterns and Different Distances. *Engineering Failure Analysis Journal*. 2025;168:109096.
13. Xu Y, Zhang H, Gan Y, Savija B. Cementitious Composites Reinforced with 3D Printed Functionally Gradedpolymeric Lattice Structures: Experiments and Modelling. *Additive Manufacturing*. 2021;39: 101887.
14. Meng Z, Xu Y, Xie J, Zhou W, Bol RJM, Liu QF, Šavija B. Unraveling the Reinforcing Mechanisms for Cementitious Composites with 3D Printed Multidirectional Auxetic Lattices Using X-Ray Computed Tomography. *Materials & Design*. 2024;246: 11331.
15. Oza RB, Kangda MZ, Agrawal MR, Vakharia PR, Solanki DM. Marble Dust as a Binding Material in Concrete: A Review. *Material Today: Proceedings*. 2022;60: 421–430.
16. Basha SA, Shaikh FUA. Suitability of Marble Powders in Production of High Strength Concrete. *Low-Carbon Materials and Green Construction* 2023;1: 27.
17. Shooshpasha I, Hasanzadeh A, Kharun M. Effect of Silica Fume on the Ultrasonic Pulse Velocity of Cemented Sand. International Conference on Engineering Systems, *Journal of Physics: Conference Series*. 2020;1687: 012017.
18. Shooshpasha I, Hasanzadeh A, Kharun M. The Influence of Micro Silica on the Compaction Properties of Cemented Sand. *IOP Conference Series: Materials Science and Engineering*. 2019;675: 012002.
19. Pereira P, Evangelista L, de Brito J. The Effect of Superplasticizers on the Mechanical Performance of Concrete Made with Fine Recycled Concrete Aggregates. *Cement and Concrete Composites*. 2012;34: 1044–1052.
20. Puertas F, Santos H, Palacios M. Polycarboxylate Superplasticiser Admixtures: Effect on Hydration, Microstructure and Rheological Behaviour in Cement Pastes. *Advances in Cement Research*. 2005;17: 77–89.
21. Husna A, Ashrafi S, Tomal AA, Tuli AT, Rashid AB. Recent Advancements in Stereolithography (SLA) and Their Optimization of Process Parameters for Sustainable Manufacturing. *Hybrid Advances*. 2024;7: 100307.
22. Melchels FPW, Feijen J, Grijpma DW. A Review on Stereolithography and Its Applications in Biomedical Engineering. *Biomaterials*. 2010;31(24): 6121–6130.
23. Patel R, Desai C, Kushwah S, Mangrola MH. A Review Article on FDM Process Parameters in 3D Printing for Composite Materials. *Materials Today Proceedings*. 2022;60: 2162–2166.
24. ASTM International. *ASTM C 109. Standard Test Method for Compressive Strength of Hydraulic Cement Mortars (Using 2-in. or [50-Mm] Cube Specimens)*. ASTM; 2017.
25. ASTM International. *ASTM International. ASTM C39/C39M-21, Standard Test Method for Compressive Strength of Cylindrical Concrete Specimens*. ASTM; 2021.

26. Jiao G, Yan G. Design and Elastic Mechanical Response of a Novel 3D-Printed Hexa-Chiral Helical Structure with Negative Poisson's Ratio. *Materials & Design*. 2021;212: 110219.
27. Rad MS, Hatami H, Ahmad Z, Karimdoost Yasuri A. Analytical Solution and Finite Element Approach to the Densere-Entrant Unit Cells of Auxetic Structures. *Acta Mechanica*. 2019;230: 2171–2185.
28. Kumar Choudhr N, Panda B, Shanker Dixit U. Energy Absorption Characteristics of Fused Deposition Modeling 3D Printed Auxetic Re-Entrant Structures: A Review. *Journal of Materials Engineering and Performance*. 2023;32: 8981–8999.
29. Levkina EV, Titova NY. The Analysis of the Financial Condition of Small Business and the Ways of its Development in the Primorsky Territory. *IOP Conference Series: Earth and Environmental Science*. 2019;272(3): 032185.
30. Shcherban' EM, Stel'makh SA, Mailyan LR, Beskopylny AN, Smolyanichenko AS, Chernil'nik AA, Elshaeva DM, Beskopylny NA. Structure and Properties of Variatropic Concrete Combined Modified with Nano- and Micro-silica. *Construction Materials and Products*. 2024;7(2): 3.
31. Hematibahar MH, Kharun M, Fediuk RS, Vatin NI, Porvadov MG, Sabitov LS. Predicting the flexural strength of 3D-printed geopolymer reinforced concrete using machine learning techniques. *Materials Physics and Mechanics*. 2025;53(4): 22–34.
32. Golias E, Schlüter FE, Spyridis P. Strengthening of Reinforced Concrete Beam-Column Joints by Means of Fastened C-FRP Ropes. *Structures*. 2024;66: 106811.
33. Chandramouli P, Jayaseelan R, Pandulu G. Axial Compression Behaviour of Hybrid Composite FRP–Concrete–Steel Double-Skin Tubular Columns with Various Fibre Orientations. *Case Studies in Construction Materials*. 2022;17: e01326.
34. Petropavlovskaya VB, Petropavlovskii KS, Novichenkova TB, Klyuev SV, Vasilev YE, Ignatyev AA. Fine-grained cement concrete with compressed structure, modified with basalt technogenic highly dispersed powder. *Construction Materials and Products*. 2025;8(4): 2.
35. Fediuk R, Smoliakov A, Muraviov A. Mechanical properties of fiber-reinforced concrete using composite binders. *Advances in Materials Science and Engineering*. 2017;2017(1): 2316347.
36. Moonphukhiao A, Samran B, Chaiwichian S. Preparation and characterization of geopolymer/activated carbon composite materials used as a bone substitute material. *Materials Physics and Mechanics*. 2025;53(1): 150–158.
37. Fediuk RS, Smoliakov AK, Timokhin RA, Batarshin VO, Yevdokimova YG. Using thermal power plants waste for building materials. *IOP Conference Series: Earth and Environmental Science*. 2018;87(9): 092010.
38. Klyuev SV, Ayubov NA, Fomina EV, Ageeva MS, Klyuev AV, Nedoseko IV. Influence of carbon black additives and finely ground waste from stone wool production on characteristics of cement systems. *Construction Materials and Products*. 2025;8(4): 8.
39. Fediuk R. Reducing permeability of fiber concrete using composite binders. *Special Topics and Reviews in Porous Media*. 2018;9(1): 79–89.
40. Ham S, Jong Han J, Kim J. Chiral Materials for Optics and Electronics: Ready to Rise? *Micromachines*. 2024;24: 528.
41. Fediuk RS, Lesovik VS, Liseitsev YL, Timokhin RA, Bituyev AV, Zaiakhanov MY, Mochalov AV. Composite binders for concretes with improved shock resistance. *Magazine of Civil Engineering*. 2019;85(1): 28–38.
42. Momeni K, Vatin N, Hematibahar M, Gebre T. Differences between 3D Printed Concrete and 3D Printing Reinforced Concrete Technologies: A Review. *Frontiers in Built Environment*. 2025;10: 145062.
43. Fediuk RS, Yevdokimova YG, Smoliakov AK, Stoyushko NY, Lesovik VS. Use of geonics scientific positions for designing of building composites for protective (fortification) structures. *IOP Conference Series: Materials Science and Engineering*. 2017;221(1): 012011.
44. Kharun M, Alaraza HA, Hematibahar M, Al Daini R, Manoshin AA. Experimental Study on the Effect of Chopped Basalt Fiber on the Mechanical Properties of High-Performance Concrete. *AIP Conference Proceedings*. 2022;2559(1): 050017.
45. Fediuk RS, Lesovik VS, Mochalov AV, Otsokov KA, Lashina IV, Timokhin RA. Composite binders for concrete of protective structures. *Magazine of Civil Engineering*. 2018;82(6): 208-218.
46. Ayoub T, Alaa Hasan H, Sheikh MN, Hadi NSM. Effect of CFRP Strip Tie Configurations on the Behavior of GFRP Reinforced Concrete Columns under Different Loading Conditions. *Structures*. 2024;69: 1072426.